EFFECTS OF ANNEALING REGIMS ON THE STRUCTURAL AND OPTICAL PROPERTIES OF INAS AND GASB NANOCRYCTALS CREATED BY ION–BEAM SYNTHESIS IN SI MATRIX

Fadei F. Komarov[1*], **Ludmila A. Vlasukova**[1], **Oleg V. Milchanin**[1],
Mikel V. Greben[1], **Alexander V. Mudryi**[2], **W. Wesch**[3]

1 Belarusian State University, Nezavisimosti ave. 4, 220030 Minsk, Belarus
2 Scientific and Practical Materials Research Center, National Academy of Sciences of Belarus, P. Brovki Str. 17, 220072 Minsk, Belarus
3 Institut für Festkörperphysik, Friedrich-Schiller-Universität Jena, Max-Wien-Platz 1, D-07743 Jena, Germany

ABSTRACT

We have studied the ion-beam synthesis of InAs and GaSb nanocrystals in Si by high-fluence implantation of (As+In) and (Ga+Sb) ions followed a thermal annealing. In order to characterize the implanted samples Rutherford backscattering spectrometry in combination with the channelling (RBS/C), transmission electron microscopy (TEM), Raman spectrometry (RS) and low-temperature photoluminescence (PL) techniques were employed. It was demonstrated that by introducing getter, varying the ion implantation temperature, ion fluences and post-implantation annealing duration and temperature it is possible to form InAs and GaSb nanocrystals in the range of sizes of (2 – 80) nm and create different types of secondary defects distribution. RS results confirm the crystalline state of the clusters in the silicon matrix after high-fluence implantation of heavy (As+In) and (Ga+Sb) ions. Significant redistribution of implanted species has been revealed after "hot" implantation and post-implantation annealing. We have suggested that it is caused by non-equilibrium diffusion. A broad band in the spectral region of 0.7 – 1.1 eV is detected in the photoluminescence spectra of the samples. The nature of this PL band is discussed.

INTRODUCTION

A silicon based optoelectronics progress is restrained because of the absence of effective light source – light emitting diode or laser. The main problem is the indirect band gap nature of silicon, resulting in inefficient light emission. InAs and GaSb are direct band-gap A^3B^5 semiconductors with a narrow band gaps about of 0.35 eV and 0.75 eV corresponds. In this case the synthesis of InAs and GaSb quantum dots inside the crystalline Si is of interest for applications in light emitting devices. Some articles were reported, where InAs nanoclusters have been formed in Si (100) by MBE-technique [1] or by means of ion implantation in SiO_2 and Si [2 – 4] followed by thermal treatment. Such

---

[*] e-mail: KomarovF@bsu.by, tel: +375(17)2124833

clusters show intense luminescence at 1.3 μm at 4–7 K. The purpose of this paper is to investigate the effect of post-implantation thermal processing on on the structural and optical properties of Si implanted with high fluence of (As+In) and (Ga+Sb) ions. In this technique, high-fluence ion implantation produces a supersaturation of one or more implanted species in the near-surface of crystalline or amorphous matrix. The embedded impurities are then precipitates out of the host by a thermal processing. Unfortunately, the results of thermal processing of implanted crystals are not only advantages like precipitation and radiation damage recovery, but also some negative consequences such as a broadening of depth concentration profiles of embedded impurity and a net loss of implanted ions because of diffusion that is favoured at elevated temperature. Thus, ($Si+A^3B^5$) is very complex structure with specific properties, which one can control by changing the size and the distribution of the precipitates by means varying the ion implantation temperature, ion fluences and post-implantation annealing duration and temperature.

METHODS OF SAMPLE MANUFACTURING AND ANALYSIS

(100) Si wafers were implanted at 25 and 500 °C subsequently with ions of the fifth (As and Sb) group and then with ions of the third (In and Ga) group of the Periodic system. Energies and doses of ions varied in the range of (170–350) keV and $(2.8–5)\times10^{16}$ cm^{-2}. Afterwards, the samples were annealed using conventional furnace annealing and rapid thermal annealing (RTA) in inert ambient in the range of temperatures of (600–1100) °C. A part of the samples implanted at the room temperature with As and In ions was additionally exposed to H_2^+ ions (100 keV, 1.2×10^{16} cm^{-2} in terms of atomic hydrogen). This procedure was performed to obtain an internal getter at a depth of about 500 nm during post-implantation annealing. In order to analyze a depth distribution of the implanted atoms as well as to evaluate a damage of implanted material, we applied Rurtherford backscattering spectrometry in combination with the channelling technique (RBS/C). RBS measurements were performed with 1.3 MeV He^+. A structure of the implanted samples was studied by means of TEM in plan-view (PV) geometry. The TEM investigations were performed using a Hitachi H-800 instrument operating at 200 keV. The samples prepared for the TEM measurements have to be transparent for probe electron beam. It is possible if this thickness does not exceed 150 – 200 nm. For this reason for detailed investigations of more deep regions into crystal bulk we combined PV-TEM preparation with the precise removal of thin layers from the face surface of sample. The optical properties of samples were investigated by Raman spectroscopy (RS) and low temperature photoluminescence (PL). Raman scattering experiments were carried out using a RAMANOR U-1000 dispersive spectrometer. The samples were excited with a laser beam of 532 nm wavelength and the scattered light was detected in backscattering geometry. Raman spectra

were recorded at room temperature within the wave number range from 90 to 600 cm^{-1}. PL spectra were taken in the spectral region of 0.7 to 2 eV. During the measurements the samples were mounted in a liquid He immersion cryostat. The 514.5 nm line of an argon ion laser was used to induce PL. The luminescence was dispersed by a 0.6 m grating monochromator and detected by a cooled InGaAs detector.

RESULTS AND DISCUSSION

The calculation of As and In, and also Ga and Sb concentrations in Si by the RBS spectra is complicated by the overlapping of peaks from corresponding impurities of III and V groups. To solve this problem, we measured RBS spectra at two angles of the incidence of He$^+$ onto the samples: 0° and 50°. It allowed us to separate peaks from As and In as well as from Ga and Sb, and calculate the depth profiles for the both implanted species. The depth profiles of the implanted ions were obtained by simulation of spectra until they coincided completely with the experimental spectra obtained at two angles of the incidence of He$^+$ onto the samples.

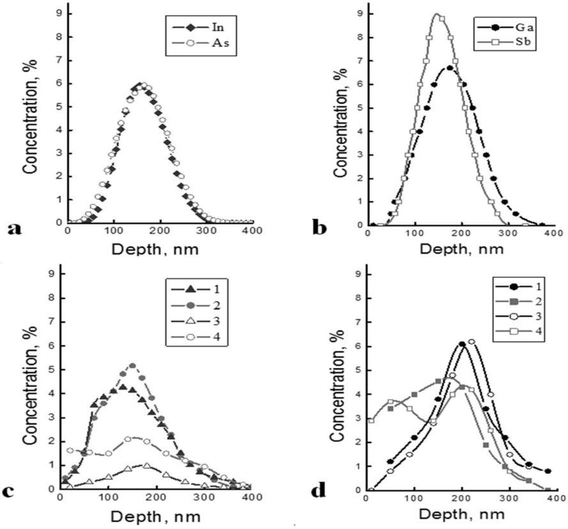

Fig. 1 – Simulated (SRIM 2010) (a – b) and calculated from the RBS spectra (c – d) depth profiles of impurities in Si, implanted with As (245 keV, 4.1×10^{16} cm^{-2}) and In (350 keV, 3.7×10^{16} cm^{-2}), and also Ga (250 keV, 5×10^{16} cm^{-2}) and Sb (350 keV, 5×10^{16} cm^{-2}) at 500 °C. As-implanted samples (c,d – 1,2) and the samples after furnace annealing at 900 °C for 60 min (c – 3,4) and for 45 min (d – 3,4): 1, 3 – In (c), Ga (d); 2, 4 – As (c), Sb (d)

Fig. 1 shows the depth As and In profiles, and also Ga and Sb atoms in the as-implanted and annealed samples. For comparison *Fig. 1a* and *Fig. 1b* depict the ion distributions calculated with the computer code SRIM'2010. It should be noted that at given ion energies the Gaussian distribution describes rather well both the theoretical (*Fig. 1a* and *Fig. 1b*) and experimental as-implanted (*Fig. 1c* and *Fig. 1d* – curves 1 and 2) depth profiles. It was mentioned in our previous work [4], that the noticeable diffusion of impurities embedded at room temperature is not revealed even under high-fluence implantation conditions. From parts (c) and (d) one can see that implantation at 500°C already leads to strong broadening and significant reduction of the impurity concentration as compared to the SRIM calculation. The As and Sb depth profiles show an asymmetric broadening towards the surface of the sample as the most effective sink for structure defects. *Fig. 1d* represents bimodal depth distribution of Sb as result of thermal annealing at 900 °C for 45 min. This effect was previously observed by authors [5] in Si implanted at 550 °C with high-fluence different types of ions and subsequently annealed at 1000 °C for 60 min. It was calculated using a numerical model [6], that embedded species redistribution experimentally observed at T_{imp}=500 °C is resulted from non-equilibrium radiation-enhanced diffusion caused by the migration of "impurity atom – radiation defect" complexes.

An analysis of the TEM data enables to receive a more detailed picture of the structure-phase transformations in the implanted layers after annealing. *Fig. 2* represents bright–field images of the precipitates for the implanted with (As+In) and annealed samples.

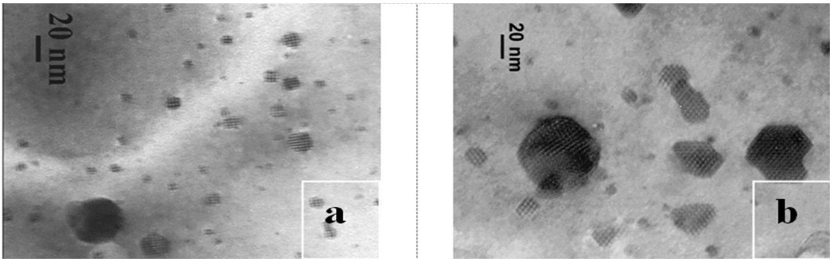

Fig. 2 – TEM plan-view images of the silicon samples implanted with As (245 keV, 4.1×10^{16} cm^{-2}) and In (350 keV, 3.7×10^{16} cm^{-2}) at 500 °C and annealed at 900 °C for 45 min (a) and 60 min (b)

It points on the presents of faceted nanoclusters with the sizes from 2 to 70 nm. The size of nanoclusters increases with boosting temperature of thermal annealing of the samples. The crystalline nature of the precipitates is proved by the presence of moiré contrast in the TEM images. It is possible to form clusters of In, As and InAs for the our experimental conditions. We have analysed the distance between the moiré bands and found out, that it is in a good agreement with the calculated one of 1.818 nm for the superposition of InAs and Si 220 planes. Thus, a layer with InAs crystallites is formed in the annealed samples. This layer is characterized by a good structural quality.

It should be noted that even at the elevated temperature applied, the high fluence of heavy Sb and Ga ions results in an essential damage of the Si crystalline lattice. The annealing does not lead to acceptable structure recovery. The surface region of the samples annealed at 900 °C for 45 min is badly damaged layer containing microtwins and precipitates (*Fig. 3*). The existence of a great number of microtwins may be caused by subsurface Sb atoms accumulation that is registered by RBS (*Fig. 1d*). Most of precipitates have a size between 10 to 60 nm. According to the RBS data a maximum of embedded atoms is located at the depth of about 200 nm. In order to investigate a structure of the implanted layer at this depth in more detail, 190 nm were removed from the surface by chemical etching for selected samples. In the thinned sample which was annealed at 900 °C for 45 min, precipitates and dislocation-like defects can be distinguished (*Fig. 3*). In order to identify nanocrystals RS was used.

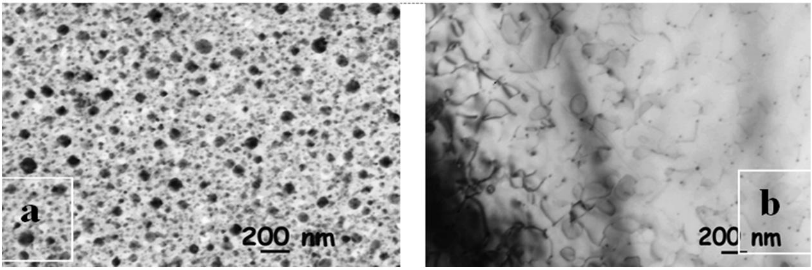

Fig. 3 – Bright-field TEM-images from silicon layers after implantation of Ga (250 keV, 5 ×10 ^{16} cm^{-2}) and Sb (350 keV, 5 ×10 ^{16} cm^{-2}) and heat treatment (900 °C, 45 min). Micrograph (b) was obtained from the thinned sample after removal the surface layer of thickness 190 nm, micrograph (a) – without removing a layer

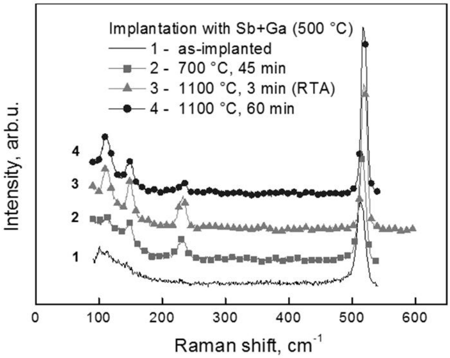

Fig. 4 – RS spectra of Si samples implanted with Sb and Ga and annealed in different modes

The Raman spectrum of an as-implanted sample (curve *1*) reveals a narrow peak at 512 cm^{-1} corresponding to zone-center phonons scattering of crystalline silicon.

The presence of this peak confirms the crystalline state of the silicon matrix after the high-fluence implantation of heavy Sb and Ga ions at elevated temperature. It should be noted than a significant shift towards low frequencies occurs in comparison with the line for undamaged Si (at 521 cm^{-1} [7]). We suggest that shift indicates an existence of significant mechanical strains within the implanted layer. Perhaps, that stress is caused of the accumulation of heavy impurity atoms (for the most part, Sb) in the sub-surface layer. Annealing leads to a shift to high frequencies (up to 518 cm^{-1} after processing at 1100 °C) and to an increase of the intensity of discussed peak. Though, tested regimes of annealing don't completely eliminate the stress in implanted layer. We have detected RS spectrum of the sample annealed at 900 °C for 45 min after etching of 190 nm-layer from its surface and registered the discussed peak position at 521 cm^{-1} (not shown). Hence, the thickness of stressed layer is lower than 190 nm. The annealing results in the appearance of additional bands in the frequency region of 110 – 235 cm^{-1}. The peak at 233 cm^{-1} is attributed to LO-phonon scattering of crystalline GaSb [7]. Its intensity changes with annealing temperature and duration and is a largest one for the sample processed at 1100 °C for 3 min. Additional peaks at 112 and 149 cm^{-1} are registered in RS spectra of annealed samples which are the characteristic lines for Sb. We attribute them to LO- and TO-phonon scattering of crystalline Sb [7]. A similar situation was reported by other authors for Si implanted with high fluence of As and In ions at 500 °C [3]. After annealing both InAs and crystalline In precipitates were detected by X-ray diffraction.

Fig. 5 depicts the PL spectra of implanted with As and In, and annealed samples. For the crystals implanted at 25 °C, a broad band in a range of 0.75–1.1 eV with a maximum of 0.93 eV is detected in PL spectra. The intensity of this band is almost five times greater for the sample with a getter layer in comparison with one without getter (curves *2* and *1* in Fig. 5, respectively). A phononless line of 0.79 eV is observed in the spectrum, due to the recombination of bound excitons on ion induced defects (interstitial carbon–interstitial oxygen (C_i–O_i pairs) [3].

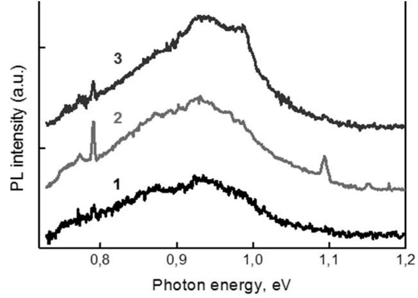

Fig. 5 – PL spectra of the silicon samples implanted with As (245 keV, 4.1×10^{16} cm^{-2}) and In (350 keV, 3.7×10^{16} cm^{-2}) and annealed at 900 °C for 60 min. T_{imp} = 25 (curves *1* and 2) and 500°C (curve *3*). The sample with getter layer – curve *2*

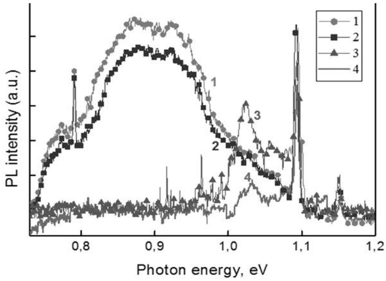

Fig. 6 – PL spectra of Si samples implanted with Ga (250 keV, 5×10^{16} cm^{-2}) and Sb (350 keV, 5×10^{16} cm^{-2}) at 500 °C and annealed in different modes: 900 °C, 3 s (1) and 45 min (2); 1100 °C, 3 min (3); 700 °C, 45 min + 900 °C, 30 s + 1100 °C, 60 min (4)

For the samples implanted at 500 °C, a broad band in the range 0.75–1.1 eV with an extended low energy wing is also found in the PL spectra (curve

3 in Fig. 5). The intensity of this band is four times greater than that of samples implanted at room temperature (*Fig. 5*, curve *1*).

PL spectra of the implanted with Ga and Sb samples are presented in *Fig.6.* One can see that a broad asymmetric band with a maximum at 0.91 eV dominates in PL spectrum. Annealing at 700 °C leads to disappearance of this band and to the appearance of an intensive band of exciton emission in Si peaked at 1.09 eV and less intensive bands at 1.03 eV and 1.14 eV. We faulted to get channelled RBS spectra from the samples annealed at 700 °C, what indicates an insufficient structural recovery of implanted layers. Therefore the implanted crystals were annealed at a temperature of 900 °C which exceeds the melting point of GaSb.

CONCLUSIONS

The influence of ion implantation and post-implantation annealing regimes on the structural and optical properties of silicon matrix with ion-beam synthesized InAs and GaSb nanocrystals has been studied. It was demonstrated that the introduction of the getter layer and varying the post-implantation annealing duration and temperature may provide the way for controlled generation of secondary defects. The InAs crystallites are mainly formed in a region of the implanted layer which is almost free of defects. A significant loss of both implanted species has been revealed as a result of "hot" implantation conditions and post-implanted annealing. A broad line at 0.7 – 1.1 eV is found in the low-temperature PL spectra of (As+In) and (Ga+Sb) implanted and annealed silicon crystals.

Acknowledgements

This work was supported by the Belarusian Republican Foundation for Fundamental Research (Grants F10R-143 and T10R-142).

REFERENCES

[1] R. Heitz, N. N. Ledentsov, D. Bimberg et al., Physica, 2000, E**7**, P. 317.
[2] F.F. Komarov, L.A. Vlasukova, O.M. Milchanin et al. Vacuum, 2005, 78**,** P. 361.
[3] A.L. Tchebotareva, J.L. Brebner, S. Roorda, C.W. White, Nuclear Instruments and Methods in Physics Research, 2001, 175-177, P. 187.
[4] F. Komarov, L. Vlasukova, W. Wesch et al. Nuclear Instruments and Methods in Physics Research, 2008, 266**,** P. 3557.
[5] A.Meldrum, J. Mater. Res., 2001, Vol. 16, P. 2670-2679.
[6] P. Zukowski, C. Karwat, F.F. Komarov et al., Phys. Status Solidi, 1996, 157, P. 373.
[7] M. Landölt, J. Börnstein, Numerical data and functional relationships in science and technology. New series, Berlin-Heidelberg: Springer-Verlag, 1982.